Effect of Linear Sequence Length on the Properties of Branched Aromatic Etherimide Copolymers

Larry J. Markoski‡ and Jeffrey S. Moore*,†,‡

Department of Chemistry and The Beckman Institute for Advanced Science and Engineering, University of Illinois, Urbana, Illinois 61801

Ibrahim Sendijarevic and Anthony J. McHugh*

Department of Chemical Engineering, University of Illinois, Urbana, Illinois 61801

Received June 23, 2000

ABSTRACT: A series of AB/AB_2 etherimide copolymers with compositions ranging from 0 to 1 mole fraction AB monomer (x_{AB}) were prepared and characterized. The weight-average molecular weight (M_w) determined from SLLS and TriSEC experiments showed good agreement. No systematic variations were found in M_w over the entire copolymer series. Rheological studies performed with concentrated solutions (10 wt % solids in NMP) showed a slight increase in viscosity with x_{AB} in the composition range 0.00−0.80 AB, followed by a sharp rise in viscosity at higher x_{AB}. The viscosity trend was closely correlated to the calculated distance between branches (l_{AB}). This observation suggests that l_{AB} is an important architectural parameter that directly affects the rheological properties of branched polymers. Similar behavior was observed for the intrinsic viscosities and Mark−Houwink coefficients measured from TriSEC in 0.05 M LiBr NMP solutions. We also observed a significant change in mechanical properties of copolymer films with $x_{AB} \geq 0.90$. Films with $x_{AB} \geq 0.90$ had the mechanical integrity to be peeled intact from a glass substrate. The glass transition temperature (T_g) showed a gradual increase with x_{AB} up to $x_{AB} \sim 0.75$, at which point a sharp rise was observed.

Introduction

Since the discovery of the unique characteristics of dendrimers[1] (e.g., monodisperse, high solubility, low viscosity, and perfectly branched geometry), researchers have sought bulk syntheses that produce dendrimer-like polymers without the cost and tedium associated with their synthesis.[2] One approach has been through the polymerization of AB_m monomers (where $m \geq 2$) to produce hyperbranched polymers in a single-pot one-step reaction, first described theoretically in 1952 by Flory.[3] This random step-growth approach produces highly branched molecules with a wide range of geometries and molecular weights. Characterization of this mixture is a necessary, albeit complex, step in trying to relate architecture and molecular weight to observed physical properties.

One of the most widely accepted terms used to describe hyperbranched polymers is the degree of branching (DB). The DB as defined by Frey[4] for an AB_2 polymerization is given by eq 1.

$$\mathrm{DB}(AB_2) = \frac{2D_{AB_2}}{2D_{AB_2} + L_{AB_2}} \qquad (1)$$

where D_{AB_2} and L_{AB_2} represent dendritic and linear segments, respectively (Figure 1). If both B groups are equally reactive and conversion of A is quite high, a DB of 0.5 will be obtained. However, hyperbranched polymers with a DB greater than 0.5 have been reported.[5−9] Since the DB is an average measure of branching and therefore molecular architecture, it would be interesting to correlate the DB to physical properties. Much effort has been put forth to create hyperbranched polymers with a DB between 0.5 and 1.0 by either slow addition techniques[6,7] or postsynthetic modification.[8] These techniques produce highly branched molecules; however, a systematic change in DB can be extremely difficult to achieve. Alternatively, the DB can be controlled between 0.0 and 0.5 in a one-pot one-step reaction through the systematic addition of AB monomers to AB_2 monomers. Surprisingly, little effort has been put forth in this area. The research that has been done has shown little correlation between DB and physical properties, mainly due to the fact that the monomers used were either structurally dissimilar[10] or the molecular weights and/or end group composition[11] varied such that no correlation could be seen. According to Frey's definition,[12] the DB of polymers synthesized by the reaction of AB + AB_2 monomers is given by eq 2.

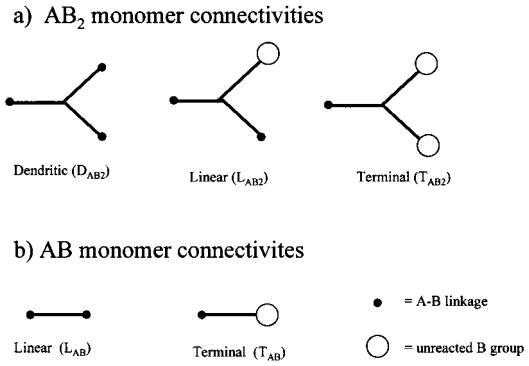

Figure 1. (a) The three types of connectivities that can be found in a hyperbranched polymer from AB_2 monomer. (b) The two possible types of connectivities in a linear polymer from AB monomer. All five repeat units can be found in random AB/AB_2 polymerizations.

† Department of Chemistry.
‡ The Beckman Institute for Advanced Science and Engineering.

10.1021/ma0010884 CCC: $20.00
Published on Web 02/28/2001

$$\mathrm{DB}(\mathrm{AB_2/AB}) = \frac{2D_{\mathrm{AB_2}}}{2D_{\mathrm{AB_2}} + L_{\mathrm{AB}} + L_{\mathrm{AB_2}}} \qquad (2)$$

where D_{AB_2}, L_{AB_2}, and L_{AB} represent the dendritic and linear segments from both the AB and AB_2 monomers, respectively (Figure 1).

We have previously communicated on the synthesis of a series of AB/AB_2 poly(etherimide) (PEI) copolymers whose dilute solution viscosities sharply increased once the composition of linear segments exceeded the 0.75 x_{AB}.[13] Herein we report full details on a series of branched poly(etherimide)s from structurally similar AB/AB_2 monomers in order to compare incremental architectural changes to physical properties such as solution rheology, film formability, and glass transition phenomena.

Experimental Section

All materials and solvents were reagent grade and were used without further purification unless noted otherwise.

^{1}H NMR spectra were taken on a Varian Unity 500 MHz spectrometer using residual solvent peak as a reference.

TriSEC[14] measurements were performed with a Waters 515 HPLC pump, a Spectraseries AS100 autosampler, a Viscotek model 300 triple detector array, and a series of three Polymer Laboratories PLgel 10um mixed B LS (7.8 × 300 mm) columns. Molecular weight data were determined using Viscotek's TriSEC software. The light scattering, mass, and viscosity constants were determined from a single 90 kDa narrow polystyrene standard and checked against other known polystyrene standards for accuracy. TriSEC data were obtained in 0.05 M LiBr NMP solutions at 65 °C.

Static Laser Light Scattering. The weight-average molecular weight, M_w, and the second virial coefficients of PEI AB/AB_2 copolymers were measured using a DAWN DSP-F laser photometer (temperature controlled by Peltier plate at 25 °C, 5 mW He−Ne laser, $\lambda = 632.8$ nm) manufactured by Wyatt Technology Corp. The M_w, radius of gyration, and second virial coefficients are related to the intensity of incident and scattered light by the following

$$\frac{Kc}{R_\theta} = \left(\frac{1}{M_w} + 2\frac{N_A B_2}{M_w^2}c\right)\left[1 + \frac{16\pi {r_g}^2}{3\lambda^2}\sin^2(\theta/2)\right] \qquad (3)$$

where K is an optical constant, c is the polymer concentration, R_θ is the Rayleigh ratio, r_g is the radius of gyration, B_2 is the second virial coefficient, and N_A is Avogadro's number. The optical constant, K, is given by

$$K = \frac{4\pi n^2(\mathrm{d}n/\mathrm{d}c)^2}{N_A\lambda^4} \qquad (4)$$

where $\mathrm{d}n/\mathrm{d}c$ is the change in refractive index with concentration and λ is the wavelength of the incident light. The M_w was determined from Zimm plots by simultaneous extrapolation of light scattering data to both zero angle and zero concentration. Since the scattering intensity of the incident light showed no angular dependence, the radius of gyration could not be determined. As is well-known,[15] this analysis yields an apparent molecular weight that, in general, will depend on the difference in the refractive index increments of the copolymer species as well as the copolymer composition. Because of their chemical similarity, we would expect the refractive index increments of the two species to be nearly the same, in which case the apparent molecular weight and weight-average molecular weight will be nearly the same. Moreover, since $\mathrm{d}n/\mathrm{d}c$ is measured for each copolymer composition, we expect our analysis to yield accurate trends related to changes in molecular weight with synthesis conditions, should they occur.

Solution Rheology. Simple shear measurements were made on a TA Instruments, AR 1000-N, constant stress rheometer using a cone and plate geometry. All experiments were conducted with a 4 cm, 2° cone that measures viscosity to an accuracy of ±3%. To prepare 10 wt % solutions, the requisite amount of polymer was dissolved in NMP with 0.05 M LiBr. A solvent trap was used to prevent evaporation, and experiments were performed at 25 °C. Temperature control was achieved with a Peltier plate (0−100 °C) to a precision of 0.1 °C.

Thermal Analysis. Differential scanning calorimetry measurements were conducted with a Mettler-Toledo DSC821^e in aluminum pans under a nitrogen atmosphere at a heating rate of 10 °C/min. Thermal gravimetric analyses were conducted with a Mettler-Toledo TGA/SDTA851^e in alumina crucibles under a nitrogen atmosphere at a heating rate of 20 °C/min.

Typical Synthetic Procedure (0.50x_{AB}). The polycondensation was performed by quickly immersing a polymerization vessel containing monomers **1** (12.54 g, 25.00 mmol) and **2** (9.29 g, 25.00 mmol) (Figure 2), a catalytic amount of cesium fluoride (150 mg, 2 mol %), and 30 mL of DMAc into a preheated 150 °C silicon oil bath. Upon stirring under a nitrogen atmosphere, the solid reagents dissolved quickly, forming a slightly yellow solution. Within about 30 s after complete dissolution, the reaction mixture began bubbling vigorously, and TBDMS fluoride evolution was observed. After the mixture was mechanically stirred for the designated time (15 min following dissolution of solids), the reaction vessel was removed from heat. While still hot, the viscous reddish solution was poured into a blender with 500 mL of absolute ethanol, followed by rapid blending. The polymer quickly precipitated, leaving a white slurry. The product was then filtered on a 2 L coarse, glass sintered funnel and washed with an additional 500 mL of ethanol and allowed to air-dry. The polymer was then dried overnight in a high vacuum oven at 100 °C to yield 14.40 g of an off-white powder (95% isolated yield). Thermal analysis showed the material to contain 3−4 wt % volatiles (solvent or water).

Results and Discussion

Synthesis. Previously, we presented[13] the syntheses of both monomers **1** and **2** (Figure 2); however, polymerization conditions for the large scale production required improvement. Initially, the solvent used for this polymerization was diphenyl sulfone (DPS) at 240 °C. This solvent is particularly inconvenient as it is a crystalline solid at room temperature. Polymerization workup required multiple precipitations to remove the residual DPS, resulting in decreased yields and possible fractionation of the final polymer. We sought a solvent that would yield the same materials at lower temperatures and could be removed easily by precipitation and drying. This change will allow for scale-up of the polymerization reaction as needed to produce sufficient quantities for bulk physical property measurements. A number of polar aprotic solvents were tested, and DMAc was found to produce high molecular weight polymer similar (Figure 3) to that produced from DPS with similar reaction times at a temperature nearly 100 °C lower than for DPS. The DMAc was easily removed with one precipitation in room temperature absolute ethanol. Subsequent drying of the polymer at 100 °C gave solids nearly free of volatiles. Thermal analysis showed that copolymers produced from the two different solvents had nearly identical glass transition temperatures. The DMAc-produced copolymers showed a 10 wt % loss at slightly lower temperatures than that of the DPS-produced copolymers, possibly due to small amounts (ca. 3−4 wt %) of residual DMAc.

Molecular Weight Determination (TriSEC and SLLS). Molecular weight was determined with triple

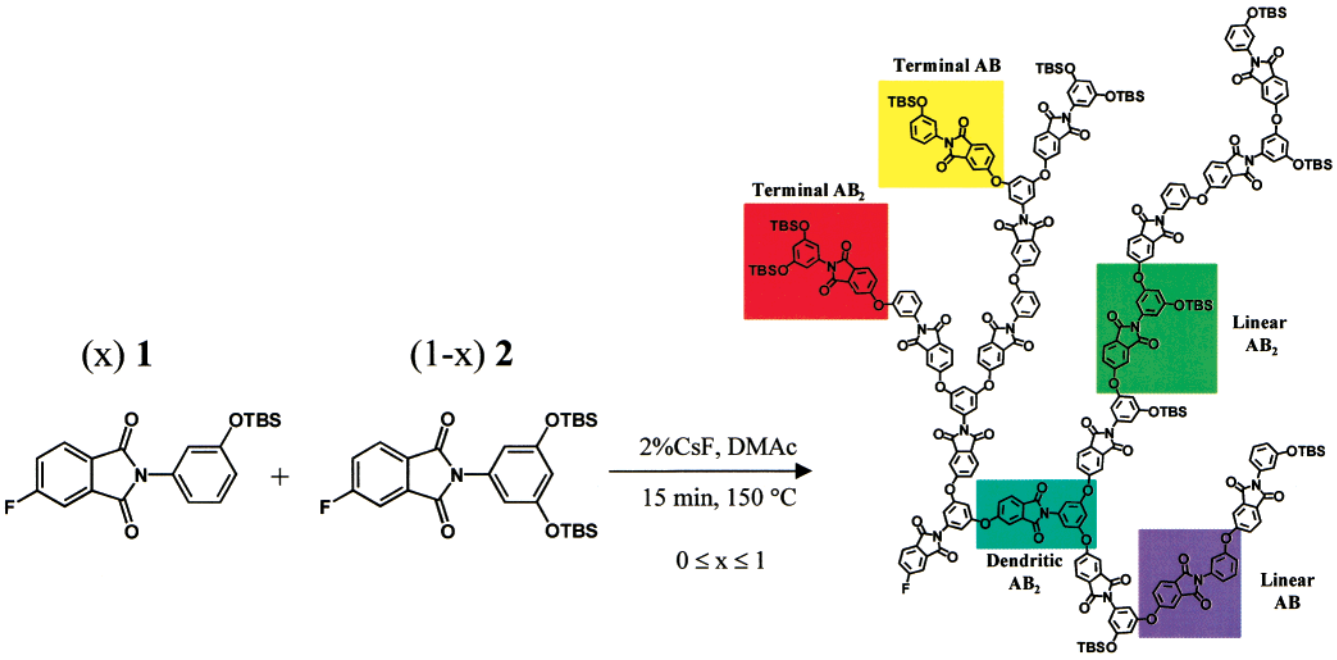

Figure 2. Schematic representation of AB/AB_2 copolymerization showing the five possible repeat units.

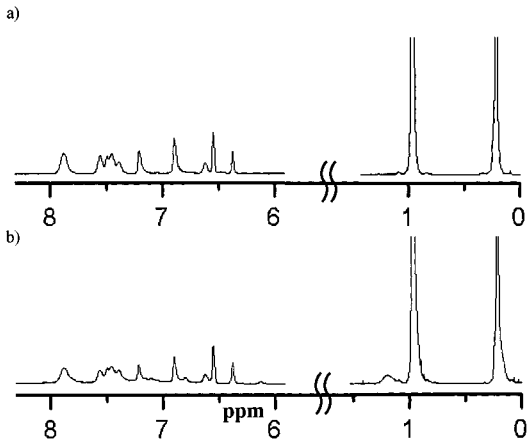

Figure 3. (a) ^{1}H NMR (500 MHz, CD_2Cl_2) of 100% AB_2 polymers polymerized in DPS. (b) ^{1}H NMR (500 MHz, CD_2Cl_2) of 100% AB_2 polymers polymerized in DMAc.

detector size exclusion chromatography (TriSEC) and static laser light scattering (SLLS). The results from the TriSEC experiments are presented in Table 1. The data show no trend in the weight-average molecular weight, M_w, as a function of the x_{AB}. However, the number-average molecular weight, M_n, decreases with increasing x_{AB}, increasing the polydispersity. This result is contrary to Flory's[3] prediction that polydispersity should decrease in random step growth polymerization with increasing x_{AB}. Our results may in part reflect unequal reactivity rates of the B and/or A groups on the monomers, intramolecular cyclization, or a polymerization mechanism that is not consistent with random step growth kinetics.

Since the TriSEC method uses a linear polystyrene standard, one might expect the molecular weights of branched polymers to be underestimated. To verify the results from the TriSEC measurements, static light scattering determinations were performed. The M_w from the SLLS are within the experimental error from values obtained by TriSEC (Table 1).

Degree of Branching. We had previously reported[13] that 0% AB and 25% AB copolymers (polymerized in DPS) had ^{1}H NMR determined DB's of 0.66 and 0.69, respectively, which is higher than the predicted 0.5 and 0.49.[12] This difference between observed and theoretical values is most likely the result of different reactivities of the B groups. However, due to aggregation or insolubility, the DB for the other members of the series could not be determined by ^{1}H NMR. More recently, when trying to measure the DB of copolymers produced from DMAc, either small losses of TBDMS end groups or small amounts of imide ring opening did not allow for the accurate ^{1}H NMR measurement of DB at high AB_2 composition. However, it is assumed that the DB of the copolymer series produced from DMAc is similar to that produced by DPS since similar physical property trends were observed for both series. Model compound studies[16] that mimicked DPS polymerization conditions showed that the DB decreases as a function of x_{AB} in a manner consistent with equal reactivity as predicted by Frey.[12]

Rheology. Figure 4 shows the steady-state shear behavior of 10 wt % solutions of the AB/AB_2 PEI copolymers in 0.05 M LiBr NMP solutions. The data display no shear rate dependence of viscosity, and no normal stress effects were observed, indicating Newtonian behavior. Hence, we assume that 10 wt % concentration solutions are sufficiently dilute such that molecular overlap and entanglements do not occur.

The effect of increasing x_{AB} on the zero-shear (Newtonian) viscosity, η_0, is shown in Figure 5. The plot suggests two distinct viscosity dependencies on x_{AB}. Initially, the data show a gradual increase in η_0 with increasing fraction of linear segments up to $x_{AB} \sim 0.80$, followed by a sharp increase in η_0 at higher fractions of linear segments. Since the viscosity is affected by the molecular architecture, an increase in viscosity with addition of linear segments suggests a change in the copolymer structure. Below a critical fraction of linear segments, where the rate of viscosity increase with x_{AB} is low, it can be inferred that changes in molecular architecture are minor. From this perspective, the

Table 1. Molecular Weight and Physical Properties of AB/AB_2 PEI Copolymers

% AB PEI copolymers	M_n[a]	M_w[a]	PDI[a]	M_w[b]	T_g (°C)	10 wt % loss (°C)	$[\eta]$ (dL/g)[a]	a[a]	yield[c]	film formation[a]
0.0	48 500	73 100	1.5	72 900	183	427	0.13	0.57	91	−
25.0	42 200	68 150	1.6	93 100	179	422	0.14	0.57	93	−
50.0	36 500	67 980	1.9	77 200	183	463	0.16	0.56	95	−
75.0	30 300	60 200	2.0	61 000	191	504	0.17	0.57	95	c
77.5	27 900	55 900	2.0	52 500	195	503	0.18	0.58	97	−
80.0	28 300	63 670	2.3	79 800	196	497	0.20	0.57	95	−
82.5	31 400	78 100	2.5	77 600	201	489	0.23	0.58	94	c
85.0	28 300	65 000	2.3	56 600	201	503	0.22	0.59	94	c
87.5	29 100	76 000	2.6	67 800	202	496	0.25	0.59	95	c
90.0	29 600	88 900	3.0	71 100	206	499	0.27	0.58	94	c, p
92.5	26 400	83 700	4.3	84 400	210	496	0.29	0.60	94	c, p, d
95.0	29 200	105 000	3.6	98 700	211	497	0.37	0.62	96	c, p, d
97.5	29 800	115 000	3.9	105 000	214	472	0.46	0.66	92	c, p, d
100.0	27 200	59 300	2.2	40 100	214	490	0.46	0.81	88	c, p, d

[a] Determined with TriSEC method in NMP (0.05 M LiBr) at 65 °C. [b] Determined with SLLS method in NMP (0.05 LiBr) at 25 °C. [c] Yield determined assuming complete conversion of A groups. [d] Films cast from 10 wt % DMAc solution at 150 °C for 30 min (−) discontinuous film, (c) continuous film, (p) film intact when peeled from glass substrate, and (d) film can be creased in half without breaking.

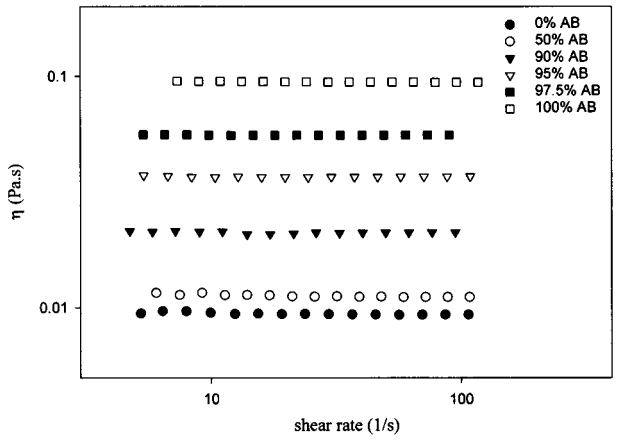

Figure 4. Simple shear viscosity as a function of shear rate for AB/AB_2 copolymers with varying fractions of AB segments at 10 wt % in 0.05 M LiBr NMP solutions and $T = 25$ °C.

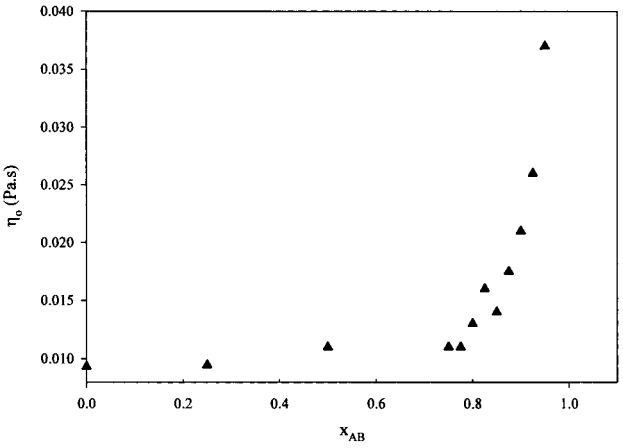

Figure 5. Zero-shear viscosity as a function of fraction of linear segments for the solutions of 10 wt % AB/AB_2 copolymers in 0.05 M LiBr NMP solutions at 25 °C.

copolymer structures with $x_{AB} < 0.80$ are similar to highly branched and rigid HBPs with $x_{AB} = 0$. In the range of $x_{AB} > 0.80$, the sharp increase in viscosity suggests that the copolymer architecture changes from a highly branched and rigid structure to one that is increasingly more linear and open.

These observations can be rationalized with the aid of predictions made by Frey and Hölter.[12] They developed the basic definitions to describe the topological changes of AB/AB_2 copolymers, based on the assumption of equal reactivity of all groups. According to their results, the probabilities of forming dendritic (D), linear (L), and terminal (T) segments from AB_2 and AB monomers are given by eqs 5 and 6.

AB_2 units:

$$p(\mathrm{D}) = p_\mathrm{A}^3 \frac{r+1}{(r+2)^2}$$

$$p(\mathrm{L}) = 2p_\mathrm{A}^2 \frac{1}{r+2}\left(1 - p_\mathrm{A}\frac{r+1}{r+2}\right)$$

$$p(\mathrm{T}) = p_\mathrm{A}\frac{1}{r+1}\left(1 - p_\mathrm{A}\frac{r+1}{r+2}\right)^2 \qquad (5)$$

AB units:

$$p(\mathrm{L}_1) = p_\mathrm{A}^2 \frac{r}{r+2}$$

$$p(\mathrm{T}_1) = p_\mathrm{A}\frac{r}{r+1}\left(1 - p_\mathrm{A}\frac{r+1}{r+2}\right) \qquad (6)$$

where r is defined as $x_{AB}/(1 - x_{AB})$ and p_A is the mole fraction of reacted A groups. By assuming complete conversion of A ($p_A = 1$), the following relations for the degree of branching (DB) and the linear sequence length or, equivalently, the average distance between branches (l_{AB}) are derived in eqs 7 and 8

$$\mathrm{DB}_{\mathrm{AB/AB_2}} = 2\frac{r+1}{(r+2)^2} \qquad (7)$$

and

$$l_{AB} = \frac{1}{2}\frac{r^2+2r+2}{r+1} \qquad (8)$$

The DB and l_{AB} are plotted in Figure 6 as a function of x_{AB}.

Similar to the observed η_0 behavior (Figure 5), the theoretical l_{AB} increases slightly with x_{AB} in the range of $x_{AB} < 0.80$, followed by a sharp increase at higher x_{AB}. The similarity in the η_0 and l_{AB} dependencies on x_{AB} suggests a possible correlation. Figure 7 shows that, in the range of $x_{AB} < 0.95$, η_0 exhibits a linear depen-

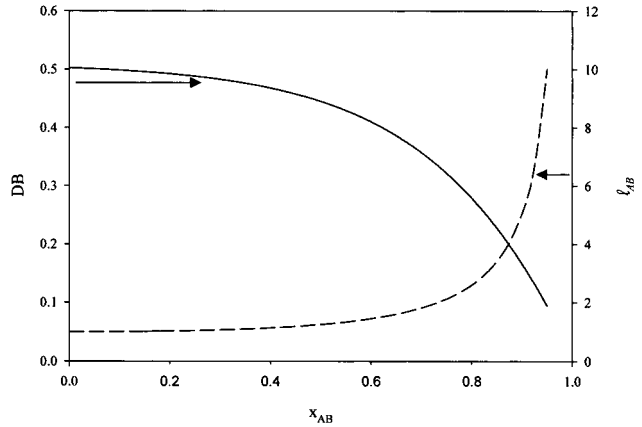

Figure 6. Distance between branches (l_{AB}) and degree of branching (DB) are plotted against the fraction of AB segments in AB/AB_2 copoymers.[12]

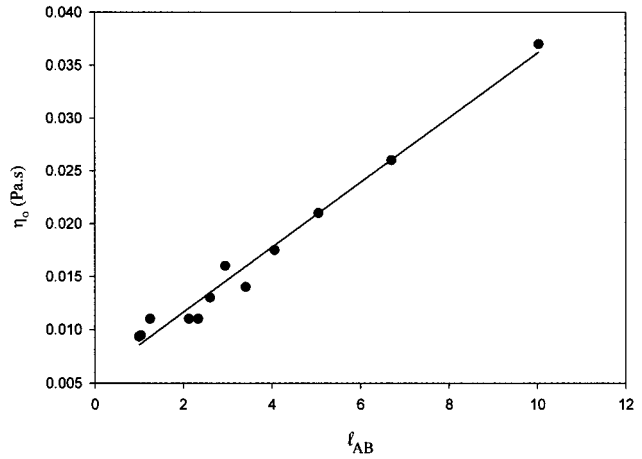

Figure 7. Zero-shear viscosity correlated to the distance between branch points for the solutions of 10 wt % AB/AB_2 copolymers of varying fractions of AB content in 0.05 M LiBr NMP solutions at 25 °C.

dence on l_{AB}. This correlation suggests that the distance between branches is an important architectural parameter that directly relates to rheological properties.

Trends similar to those shown by the simple shear data were also observed in the intrinsic viscosity measurements [η_0] from TriSEC. The [η_0] data and the Mark−Houwink−Sakurda coefficient, *a*, are presented in Table 1. The data exhibit the general trend of increasing [η_0] with increasing x_{AB}. As seen in Figure 8, direct correlation between [η_0] and l_{AB} holds in the range of $x_{AB} \leq 0.95$.

As seen in Figure 9, the Mark−Houwink−Sakurda coefficient *a* increases as the backbone of the polymer becomes less branched by the addition of linear segments. In general, *a* is expected to decrease with increasing branching of polymers. Burchard[17] shows a decrease in *a* with the addition of branches to a linear polyimidazole backbone. Frechet[18] also presented similar data for HBP and linear polymers, which clearly show lower *a* values for HBP polymers. At $x_{AB} \sim 0.80$, a sharp increase in the value of *a* is observed, which once again suggests a change in architecture at this point from a highly branched to a much more linear structure.

Thermal Properties. The glass transition temperature (T_g) of linear polymers is commonly believed to be a function of the long-range segmental motion of the polymer chain segments.[19,20] For linear polymers, the

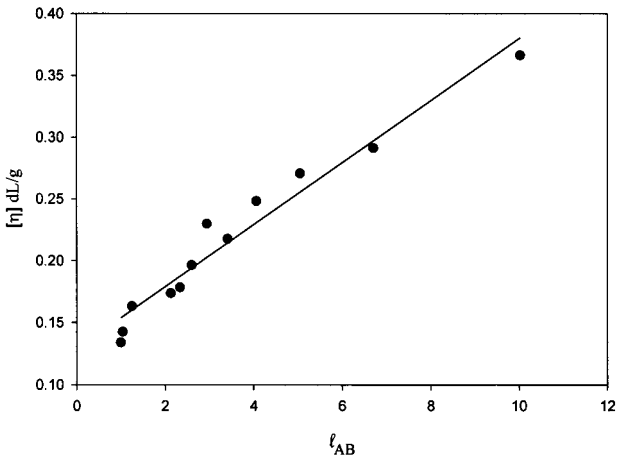

Figure 8. Intrinsic viscosity correlated to the distance between branches for AB/AB_2 copolymers of varying fractions of AB segments.

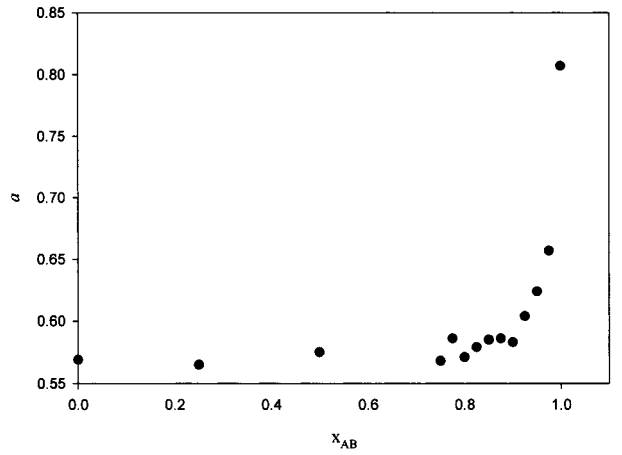

Figure 9. Mark−Houwink coefficient *a* as a function of fraction of AB segments for AB/AB_2 copolymers in 0.05 M LiBr NMP solutions at 65 °C.

effect of end groups on the T_g diminishes with an increasing degree of polymerization. However, with dendritic polymers, the number of end groups is directly proportional to the degree of polymerization, and therefore the effect of end groups on the fractional free volume and T_g can be significant, even at high degrees of polymerization. A modified Flory-type model that accounts for the free volume of end groups in dendrimers was developed by Wooley et al.[21] By assuming a constant free volume per end group, they derived the following relation shown in eq 9,

$$T_g = T_{g,\infty} - K\left(\frac{n_e}{M}\right) \tag{9}$$

where $T_{g,\infty}$ is the limiting value of the T_g for an infinitely large dendrimer, and n_e is the number of end groups for a dendrimer polymer with a molecular weight, *M*. This relation successfully captures the T_g behavior as a function of molecular weight for poly(benzyl ether) dendrimer polymers.[21] However, with randomly branched polymers, additional factors not accounted for in eq 7 also affect T_g (such as different degrees of branching, steric hindrance, and varying number of end groups). Since to our knowledge, there is no model that completely predicts the T_g of randomly branched systems, our discussion will primarily focus on a qualitative description of the competing effects on T_g.

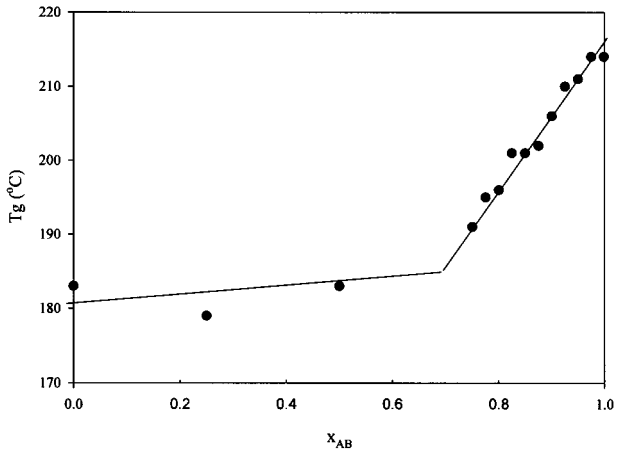

Figure 10. Glass transition temperature as a function of fraction of AB segments for AB/AB_2 copolymer.

As the monomer ratio is varied, in addition to the changing number of end groups, branching and therefore mobility of the interior of the molecule will change as well. According to Stutz,[22] unreacted end groups increase the free volume and therefore the mobility of the molecule, thus leading to a decrease in T_g. On the other hand, branch points or cross-links have the effect of reducing the mobility of the surrounding polymer chain segments, hence increasing the T_g. As a consequence, increasing the fraction of AB segments in an AB/AB_2 copolymer results in two opposing effects on the T_g. First, the number of unreacted end groups decreases, increasing the T_g, and second the number of branch points decreases, decreasing the T_g. The data in Figure 10 show an increase in values of T_g with x_{AB}, suggesting an overall decrease in mobility. Furthermore, a break in the dependence of T_g on x_{AB} at 0.70 AB is observed.

A possible explanation for the decrease in mobility with AB segments is that the number of unreacted end groups is decreasing at a faster rate than the number of branched units, thus causing an increase in the T_g. For the AB/AB_2 copolymer with a degree of polymerization of 100, Frey's theory predicts a reduction of end groups from 102 to 2 and number of dendritic segments from 25 to 0 with x_{AB} increasing from 0 to 1. Assuming a constant volume for the end groups and branch units, the free volume lost due to the decrease of end groups would be greater than the free volume gained due to a decrease of branch units, thereby decreasing the mobility and increasing the T_g. However, this analysis does not explain a sharp increase in the T_g at 0.75 AB, so additional factors must be considered. Our viscosity data suggest an abrupt change from a highly branched to a much more open and linear structure at roughly the same composition where the T_g dependency changes. In the range of $x_{AB} < 0.75$, the molecular architecture is highly branched, and the mobility of the internal structure is expected to be very low. In addition, due to steric hindrance, entanglement formation is unlikely. As suggested by Kim and Beckerbauer,[19] the main relaxation mode for highly branched polymers is the translational motion of the polymer molecule rather than the segmental chain motion, usually assumed for linear polymers. However, for $x_{AB} > 0.70$, the polymer structure becomes increasingly more open, allowing for a higher degree of molecular interpenetration and entanglement formation. By analogy to a cross-link, an entanglement is expected to reduce the free volume, thereby lowering the mobility and increasing the T_g.[23] Since a higher degree of entanglement is anticipated for the AB/AB_2 copolymers with higher content of AB units, an increase in the T_g can be expected.

Turner[23] showed that Flory's prediction for the glass transition temperature could be extended to include a contribution from entanglements as shown in eq 10.

$$T_g = T_{g,\infty} - \left(\frac{\rho N}{\alpha}\right)(\theta_1 + n_e\theta_2)(1/M) \quad \text{for } M \geq 2M_e \quad (10)$$

where θ_1 represents free volume reduced by entanglements and θ_2 free volume of the end group and M_e the critical entanglement molecular weight. From this correlation it is possible to calculate the entanglement density for polymers of $M \geq 2M_e$; however, the AB/AB_2 copolymers of various molecular weights needed for this analysis were unavailable in this study.

Conclusion

In this study we presented the synthesis and characterization of poly(etherimide) AB/AB_2 copolymers. By varying the ratio of starting monomers, polymers were synthesized with geometries ranging from fully hyperbranched (100% AB_2) to fully linear (100% AB). The differences in molecular architecture due to changes in monomer ratios were shown to affect the properties of the copolymers. As expected, an increase in viscosity was observed with increasing fraction of AB segments. Our data show small changes in viscosity for copolymers with $x_{AB} \leq 0.80$, suggesting that molecules in this range have similar highly branched structures. However, at $x_{AB} > 0.80$ sharp increases in the viscosity suggest that the molecular structure is becoming increasingly more linear and open, resembling long chain branched molecules. Viscosity changes appear to directly correlate with calculated distance between branches. A similar dependence was also observed with intrinsic viscosity measurements. These observations suggest that the distance between branches is a key architectural parameter that directly correlates to rheological properties. In addition, the changes in architecture resulting from increased distance between branches may also explain the observed improvement in mechanical properties of films with $x_{AB} \geq 0.90$.

Glass transition temperatures were found to increase with increasing fraction of AB monomers, indicating an overall decrease in mobility as the chains become more linear. Below $x_{AB} \leq 0.75$, small changes in the T_g were observed with changes in x_{AB}. In this range, where the molecular architectures are very similar, it can be inferred that due to lack of entanglements and low mobility of the interior of the molecule, the main relaxation mode is the translational motion of the polymer molecule. On the other hand, in the range of $0.75 < x_{AB} < 1.0$, a sharp increase in the T_g is observed with an increase in x_{AB}. In this range, the structure becomes increasingly more open, allowing for a higher degree of entanglement formation that reduces mobility, thus increasing the T_g.

To isolate the effects of architecture, a series of branched polymers with constant number of end groups and varying architecture are currently being investigated.

Acknowledgment. This work has been supported under a grant from the U.S. Army Research Office under Contract/Grant DAAG55-97-0126. Ibrahim Sendi-

jarevic thanks Prof. Zukoski, Amit Kulkarni, and S. Ramakrishan for their help with static laser light scattering and Matt Liberatore for his help with viscosity measurements.

References and Notes

(1) Fischer, M.; Vögtle, F. *Angew. Chem., Int. Ed.* **1999**, *38*, 884.
(2) For comprehensive reviews of the literature prior to 1998, see: (a) Malström, E.; Hult, A. *J. Macromol. Sci., Rev. Macromol. Chem. Phys.* **1997**, *C37*, 555. (b) Kim, Y. H. *J. Polym. Sci., Part A: Polym. Chem* **1998**, *36*, 1685.
(3) (a) Flory, P. J. *J. Am. Chem. Soc.* **1952**, *74*, 2718. (b) Flory, P. J. *Principles of Polymer Chemistry*; Cornell University Press: Ithaca, NY, 1953.
(4) Hölter, D.; Burgath, A.; Frey, H. *Acta Polym.* **1997**, *48*, 30.
(5) Thompson, D. S.; Markoski, L. J.; Moore, J. S. *Macromolecules* **1999**, *32*, 4764.
(6) Sunder, A.; Hanselmann, R.; Frey, H.; Mullhaupt, R. *Macromolecules* **1999**, *32*, 4240.
(7) Lach, C.; Frey, H. *Macromolecules* **1998**, *31*, 2381.
(8) Guan, Z.; Cotts, P. M.; McCord, E. F.; McLain, S. J. *Science* **1999**, *283*, 2059.
(9) Bharathi, P.; Moore, J. S. *Macromolecules* **2000**, *33*, 3212.
(10) Jayakannan, M.; Ramakrishnan, S. *J. Polym. Sci., Part A: Polym. Chem.* **2000**, *38*, 261.
(11) (a) Kricheldorf, H. R.; Stukenbrock, T. *Polymer* **1997**, *38*, 3373. (b) Kricheldorf, H. R.; Zhang, Q.; Schwarz, G. *Polymer* **1982**, *23*, 1820.
(12) Frey, H.; Hölter, D. *Acta Polym.* **1999**, *50*, 67.
(13) Markoski, L. J.; Thompson, J. L.; Moore, J. S. *Macromolecules* **2000**, *33*, 5315.
(14) Haney, M. A.; Gillespie, D.; Yau, W. W. *Today's Chemist at Work* **1994**, *3*, 39.
(15) Yamakawa, H. *Modern Theory of Polymer Solutions*; Harper and Row: New York, 1971.
(16) Markoski, L. J.; Thompson, J.; Moore, J. S., unpublished results.
(17) Burchard, W. *Adv. Polym. Sci.* **1999**, *143*, 113.
(18) Fréchet, J. M. J. *J. Macromol. Sci., Pure Appl. Chem.* **1996**, *A33*, 1399.
(19) Kim, Y. H.; Beckerbauer, R. *Macromolecules* **1994**, *27*, 1968.
(20) Hult, A.; Johansson, M.; Malmström, E. *Adv. Polym. Sci.* **1999**, *143*, 1.
(21) Wooley, K. L.; Hawker, C. J.; Pochan, J. M.; Fréchet, J. M. J. *Macromolecules* **1993**, *26*, 1514.
(22) Stutz, H. *J. Polym. Sci., Part B: Polym. Phys.* **1995**, *33*, 333.
(23) Turner, D. T. *Polymer* **1978**, *19*, 789.

MA0010884